Fragmentation of isoxazole molecules by electron impact

in the energy range 10-85 eV

Ireneusz Linert, Izabela Lachowicz, Tomasz J. Wasowicz, Mariusz Zubek

Department of Physics of Electronic Phenomena, Gdańsk University of Technology,

80-233 Gdańsk, Poland

Abstract

Fragmentation of isoxazole molecules by electron impact excitation, that produces excited atomic and molecular fragments, has been studied using the optical excitation technique. Excited hydrogen atoms H(n), n = 4-7, have been detected by observation of the H_β to H_ϵ lines of the Balmer series. The diatomic $CH(A^2\Delta)$ and $CN(B^2\Sigma^+)$ fragments have been identified by their $A^2\Delta \rightarrow X^2\Pi_r$ and $B^2\Sigma^+ \rightarrow X^2\Sigma^+$ emission bands, respectively. The appearance energies for the H(n=4), $CH(A^2\Delta)$ and $CN(B^2\Sigma^+)$ have been measured to be 21.9, 14.0 and 10.6 eV, respectively. Absolute emission cross sections have been also obtained for the fragments in electron energy ranges from their respective appearance thresholds up to 85 eV. Possible fragmentation processes are discussed.

Keywords: Fragmentation processes, Electron impact, Dissociative excitation,

Fluorescence emission.

Corresponding author E-mail: mazub@mif.pg.gda.pl

1. Introduction

Dissociation and fragmentation of polyatomic molecules are fundamental processes which may be initiated by absorption of radiation or by electronic collisions. Such molecular processes can be uncovered by a combination of experimental spectroscopic measurements and *ab initio* theoretical investigations. In recent years, much attention has been paid [1-6] to studies of nonradiative deactivation of lower lying excited states of five-membered heterocyclic aromatic molecules, furan (C_4H_4O), pyrrole (C_4H_4NH), thiophene (C_4H_4S) (see Fig. 1) and their derivatives. The above ring molecules serve as analogues of structural building blocks of biologically important molecules and play significant roles in the syntheses of biologically active compounds and organic polymers. These studies show that fragmentation of five-membered heterocyclic molecules is one of the efficient channels of their deactivation. For example, deactivation processes of photoexcited states of pyrrole involve hydrogen atom detachment which is the main dissociation channel after excitation into both the lowest dissociative $^1\pi\sigma^*$ and bound $^1\pi\pi^*$ states [1]. Production of H atoms from the $^1\pi\sigma^*$ state is due to direct adiabatic N-H bond cleavage and to ultrafast internal conversion from the $^1\pi\sigma^*$ excited state to the ground state through conical intersection with subsequent unimolecular dissociation [1,2]. A new deactivation mechanism based on the out-of-plane ring deformation which directly couples the $^1\pi\pi^*$ and the ground states has been proposed [3]. This mechanism should create slow H atoms and additionally HCN and CNH_2 fragments via ring opening mechanism. Deactivation via a ring opening has been also found in the combined Kohn-Sham density functional and multi-reference configuration interaction calculations carried out for furan [4] and thiophene [5]. The ring opening mechanism may also lead to fragmentation of furan and thiophene molecules [6].

In this work we explored electron impact induced fragmentation processes of the gas-phase isoxazole (C_3H_3NO) molecule which result in formation of excited neutral atomic and molecular fragments. The optical excitation technique was applied which allowed identification of the dissociation and fragmentation species by detection of their fluorescence decay. Isoxazole is isoelectronic to furan and pyrrole and as a heterocyclic molecule contains one oxygen and one nitrogen heteroatom (Fig. 1).

Previously, fragmentation of isoxazole molecules were investigated by Lifshitz and Wohlfeiler [7] who used a single-pulse shock tube in thermal decomposition over the temperature range 850-1100 K. These investigations found that acetonitrile $CH_3C\equiv N$ and carbon monoxide CO are the major products of decomposition accompanied by several minor products which include hydrogen cyanide HCN and ketene CH_2CO. It has been suggested [7] that formation of $CH_3C\equiv N$ and CO involves a unimolecular process of a concerted N-O bond cleavage, H atom migration from position C(5) to C(4), and a cleavage of a C(4)-C(5) bond followed by removal of CO from the ring. The two decomposition channels leading to formation of CO and HCN were studied in theoretical calculations [8,9]. Okada and Saito [8] concluded that the major products were formed by bifurcation due to a dynamical effect in the thermal decomposition. The density functional and *ab initio* calculations of Higgins et al. [9], however, indicated that the decomposition mechanism of isoxazole proceeds through an intermediate state of open-ring geometry $N\equiv CCH_2CHO$. Production of CH_3CN and CO requires migration of an H atom from the position C(5) to C(4) and a cleavage of the C(4)-C(5) bond. Furthermore, in high-level *ab initio* and semi-empirical computational studies Davico [10] investigated the mechanisms of thermal isomerization of isoxazole and pointed out that it can take place at lower temperatures (<850 K) than, for example, the decomposition process leading to the azirine isomer.

Decomposition processes of isoxazole positive ions produced by electron impact were studied by Bouchoux and Hoppilliard [11]. The main fragment ions revealed in their mass analyzed spectra are: $C_3H_2NO^+$ formed by loss of an H atom, $C_2H_3N^+$ resulting from loss of CO and $C_2H_2N^+$ obtained from loss of HCO. Production of the above ions was explained implying isoxazole heterocyclic ring opening by cleavage of the N-O bond and migrations of H atoms [11]. Dissociative electron attachment to isoxazole molecules, which generates stable negative ions and neutral fragments was reported by Walker et al. [12] in the electron energy range 0-10 eV. These authors measured the total negative ion signal, without mass analysis of the detected ions.

In the present work, the following fragmentation species have been observed: hydrogen H(n), n = 4-7, and diatomic CH($A^2\Delta$), CN($B^2\Sigma^+$) and $C_2(d^3\Pi_g)$ fragments. These atomic and molecular products differ from those previously reported in isoxazole [7] indicating major differences between electron impact and thermal dissociation. Their identification gives new insight into dissociation and fragmentation channels of the excited states of isoxazole which are in the energy region above the first ionization threshold (9.976 eV). The appearance energies for the H(n=4), CH($A^2\Delta$) and CN($B^2\Sigma^+$) have been measured to be 21.9 ± 0.5, 14.0 ± 0.4 and 10.6 ± 0.4 eV, respectively. Absolute emission cross sections have been also determined for the above three fragments in the electron energy range from their respective appearance thresholds up to 85 eV.

2. Experimental

The measurements were performed using the electron impact optical excitation technique, employing an electron spectrometer which was described in detail previously [13]. Briefly, electrons emitted by a tungsten filament are collimated into a beam by a trochoidal selector and a set of adjacent aperture electrodes. Before entering the collision region the electrons are accelerated to the required energy in the range 10-85 eV. The

MOST WIEDZY Downloaded from mostwiedzy.pl

electron beam is directed along the spectrometer by a magnetic field of 60-80 Gauss produced by two coils. The direction of the magnetic field is adjusted to coincide with the spectrometer axis. The electron beam leaving the collision region is monitored by a collector. Its intensity was in the range 1-4 µA and was constant over the energy range of the measurements to within ±10%. The energy spread of the beam was estimated to be 400 meV (FWHM). Fluorescence emission from the collision region passes through a quartz light-guide and is focused on the entrance slit of the 0.25 m Ebert monochromator equipped with a grating having 1181 lines/mm. A cooled photomultiplier is used to detect the transmitted radiation.

In the first step of the measurements, fluorescence emission spectra were obtained in the 330-530 nm wavelength range for fixed electron energies. In these measurements the optical resolution ($\Delta\lambda/\lambda$) was 0.0035. The wavelength scale was calibrated to ±0.2 nm in nitrogen against the position of the (0,0) line (337.0 nm) of the second positive band. The recorded spectra were corrected for the wavelength variation of sensitivity of the optical detection channel. The wavelength variation of the relative sensitivity of the photon detection channel was determined by applying method of the molecular branching ratio. The details of the method and the molecular bands used in the procedure were described previously [14]. In the second part of this work, excitation functions for selected optical bands were obtained in given electron energy ranges. It is estimated that the collision path length in the interaction region varied as a result of the helical motion of electrons in the magnetic field by less than 10% over the energy range 10-85 eV. In the measurements of the excitation functions in the above energy range the spectrometer was tuned to ensure low changes of the electron current with the increasing electron energy. These changes were typically ±4% as monitored by electron collector and were not used to correct the photon signal. Special attention was paid to measurements close to threshold regions to

5

determine the appearance energies of detected emissions. During the whole experiment care was taken to maintain conditions of linear dependences of photon signals on target gas pressure and intensity of the incident electron beam to avoid collisional quenching of excited fragments, trapping of emitted radiation and double electron collisions. The incident electron energy was calibrated against the position of the excitation threshold of the 337 nm line at 11.03 eV in a mixture of isoxazole and nitrogen.

Emission cross sections were measured for the H_β line and $CH(A^2\Delta \rightarrow X^2\Pi_r)$ and $CN(B^2\Sigma^+ \rightarrow X^2\Sigma^+)$ bands of isoxazole in the energy range 10-85 eV. To obtain absolute values, the relative cross section for the H_β line was normalized at 60 eV against the apparent emission cross section of the 388.9 nm (3^3P-2^3S) line in helium measured by van Raan et al. [15]. Here, the intensities of the H_β and helium lines were compared which were measured in both gases at known electron beam currents and absolute gas pressures in the collision region. The $CH(A^2\Delta \rightarrow X^2\Pi_r)$ and $CN(B^2\Sigma^+ \rightarrow X^2\Sigma^+)$ cross sections which include rotational and vibrational excitation of the fragments were determined by comparing the areas under the corresponding bands (see 3.1) and the H_β line in the fluorescence spectrum measured at 60 eV assuming a smoothly varying background between the bands. The polarization of the helium 388.9 nm line is 15% at 60 eV [16] and that of molecular fluorescence in dissociation is typically less than 5%. Thus the possible polarization effects in the present measurements are small and were neglected. The total uncertainty in the absolute H_β emission cross section was estimated to be 40% taking an uncertainty in the helium emission cross section of 15%. The uncertainties in the CH and CN emission cross sections further include contributions from the uncertainties in the peak area ratios of 10% and they reach 50%.

Isoxazole purchased from Aldrich with a declared purity of 99% was degassed several times under vacuum to remove any gaseous impurities before any measurements were taken.

3. Results and discussion

3.1 Emission spectrum and cross sections

The fluorescence spectrum of isoxazole measured at the electron energy of 70 eV and in the wavelength range of 330-525 nm, with a resolution of 1.0-1.4 nm is shown in Fig. 2. The prominent features of the spectrum are the $A^2\Delta \rightarrow X^2\Pi_r$ and $B^2\Sigma^+ \rightarrow X^2\Sigma^+$ (violet system) emission bands of the excited $CH(A^2\Delta)$ and $CN(B^2\Sigma^+)$ fragments, respectively. The CH band at 430 nm is asymmetric on the low wavelength side and broadened at the base which extends from 415 nm to 440 nm. This shape of the CH band arise from overlapping series of rotational lines of the (0,0), (1,1) and (2,2) vibrational transitions. The increased width at the base indicates high rotational excitation of the CH fragments which may be inferred from comparison with similar CH emission spectra measured in the dissociation of ethane by electron and also fast argon ion impact [17]. High optical resolution in these works allowed rotational lines to be resolved and simulations of the spectra gave a rotational temperature of 4000 K for the v´=0 level of the $CH(A^2\Delta)$, which had the highest population [17]. The CN emission bands emerge between 375-390 nm ($\Delta v=0$) and 350-362 nm ($\Delta v=-1$) and show vibrational (v'=0-4) and rotational excitation of the CN fragments [18]. The weak structures at 363 nm and above 390 nm we attribute to emission from the $CH(B^2\Sigma^-)$ excited state. Much weaker molecular bands due to the vibrationally excited $C_2(d^3\Pi_g)$ ($d^3\Pi_g \rightarrow a^3\Pi_u$, Swan system) are detected near 468 nm and 510 nm. The fluorescence spectrum of Fig. 2 also contains four atomic lines of the Balmer series, H_β through to H_ε arising from the loss of a hydrogen H(n) atom in the n=4-7 states. The intensity of these lines are plotted as a function of the n principal quantum number in

7

Fig. 3 and are approximated by an n^{-k} exponential function, where k is a constant. The least-squares fitting gave the constant k equal to 3.57 ± 0.03. The intensities of the emission lines in the hydrogen series for the (n,l) excited substates populated according to their statistical weights $(2l + 1)$ decrease as n^{-3} with increasing n to better than 5% [19]. This dependence was previously observed in studies of the dissociation of some heavier aliphatic hydrocarbons for the Balmer series [20] and of silane for the Lyman series [21]. Our k value may indicate that the hydrogen $H(n,l)$ dissociation fragments in isoxazole are populated approximately according to their statistical weights and further that they are produced from a number of higher-lying (superexcited) states of isoxazole excited by electron collisions. The molecular bands and atomic lines of the fluorescence spectrum of Fig. 2 are superimposed on a smoothly varying background which may be produced by excited polyatomic fragments of isoxazole.

The isoxazole fluorescence spectrum may be compared with that measured in furan at 70 eV in very similar studies performed in our laboratory [13]. The $CH(A^2\Delta)$ emission band of isoxazole displays a nearly identical shape to that of furan. The line intensities of the Balmer series in isoxazole decrease slightly faster with n than that of furan where we found $k = 3.2 \pm 0.3$. Furthermore, the $C_2(d^3\Pi_g)$ bands in isoxazole have much lower intensities than those of furan.

The emission cross section determined for the $CH(A^2\Delta \rightarrow X^2\Pi_r)$ band in the 10-85 eV energy range is shown in Fig. 4. The measurements were carried out at 430 nm in a bandwidth of 2.5 nm, while the background was determined at 450 nm and was subtracted from the 430 nm intensity. The appearance energy for the $CH(A^2\Delta)$ fragment was found to be 14.0 ± 0.4 eV and the threshold region of the emission cross section is shown in the inset of Fig. 4. Fig. 5 displays emission cross sections of the $CN(B^2\Sigma^+ \rightarrow X^2\Sigma^+)$ band and the H_β line. The CN cross section was measured at 385 nm using 3.0 nm bandwidth while

the background was determined at 370 nm. The measurements of the appearance energies of the CN($B^2\Sigma^+$) and H(n=4) fragments gave values of 10.6 ± 0.4 eV (see inset of Fig. 5) and 21.9 ± 0.5 eV, respectively. The CH($A^2\Delta$) appearance energy obtained in isoxazole is much lower than that determined in furan (19.0 ± 0.3 eV [13]), while the present appearance energy of the H(n=4) is comparable to that of furan (20.7 ± 0.4 eV). The emission cross sections in both molecules have similar values in the 80-90 eV energy region.

3.2 Fragmentation processes of isoxazole

The appearance energies of the observed fragmentation species are above the adiabatic ionization energy of isoxazole, which was measured at 9.976 eV [22]. In the fragmentation process the higher-lying (superexcited) states of the molecule are excited and next undergo decomposition following energetically and dynamically favourable routes on the hyperdimensional potential energy surface. Estimation of the fragmentation energy limits and a comparison with the measured appearance energies allows to suggest most probable molecular processes leading to the detected species. Formation of the CN($B^2\Sigma^+$) fragment, which has the lowest appearance energy (10.6 eV) of the three studied species requires opening of the ring of the isoxazole molecule by cleavage of the N-O bond and further breaking of the C(3)-C(4) bond producing the final products

$$C_3H_3NO^* \rightarrow \cdot CH_2HC{=}O + CN(B^2\Sigma^+). \qquad (1)$$
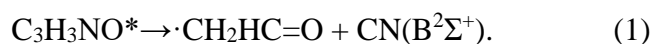
In the opening of the ring, the N≡C triple and C=O double bonds are formed accompanied by the H atom migration from the C(3) to C(4) carbon atom. The fragmentation energy limit for the above reaction is estimated to be 7.36 eV. In this estimation, for the open structure of isoxazole the linear nitrile N≡CCH$_2$HC=O isomer has been taken which potential energy has been found in the MP2/cc-pVDZ calculations [10] to be 1.11 eV (25.57 kcal/mol) below that of the ring structure. Furthermore, the CH$_2$-CN bond

9

dissociation energy is 5.28 eV [23] and the excitation energy of the $CN(B^2\Sigma^+)$ v=0 vibrational level is 3.19 eV. The excess energy of 3.2 eV above the fragmentation limit in (1) will be shared between rotational and vibrational excitation of CN, excitation of the second fragment and translational energies of both fragments. Further dissociation of the $\cdot CH_2HC=O$ fragment in (1) by C(4)-C(5) bond cleavage is also energetically allowed as it requires about 2.8 eV. However, abstraction of H or O atoms accompanying (1) have fragmentation energy limits above the measured appearance energy. It is interesting to note that in the recent measurements of electron energy loss spectra [24] an electronic band at 10.6 eV has been seen which may be the initial excited state in the dissociation process (1).

Production of $CH(A^2\Delta)$ involves multiple fragmentation of the linear nitrile $N\equiv CCH_2HC=O$ isomer including detachment of CN. The lowest fragmentation energy limit of 10.5 eV is obtained for the process

$$C_3H_3NO^* \rightarrow CH_2O + CN + CH(A^2\Delta) \qquad (2)$$
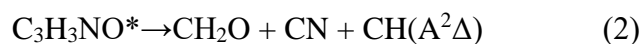
where the formaldehyde molecule, CH_2O is formed by migration of one of the H atoms from C(4) to C(5) and cleavage of the single C(4)-C(5) bond which requires a total energy of 3.5 eV. This energy is deduced from known dissociation energies of the molecular bonds involved [23]. The excitation energy of the $CH(A^2\Delta)$ v=0 level is 2.88 eV. Process (2) which apart from the excited $CH(A^2\Delta)$ fragment will also produce excited $CN(B^2\Sigma^+)$ has an estimated energy limit of 13.8 eV, which is close but below our measured appearance energy of 14.0 eV. Two other processes which give rise to radicals

$$C_3H_3NO^* \rightarrow \cdot CH_2CN + O + CH(A^2\Delta) \qquad (3)$$

$$C_3H_3NO^* \rightarrow \cdot COH + CN + H + CH(A^2\Delta) \qquad (4)$$
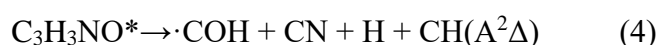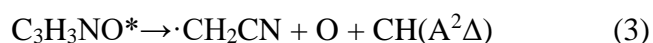
are likely to occur, at least considering their fragmentation energy limits of 13.0 eV and 13.8 eV, respectively. The appearance energy measured in isoxazole for the CH($A^2\Delta$) fragment is 5 eV lower than that in furan [13].

The hydrogen H($n=4$) atom may be directly eliminated from one of the C-H bonds in the closed ring of isoxazole (Fig. 1)

$$C_3H_3NO^* \rightarrow C_3H_2NO + H(n=4). \tag{5}$$

For the three C(3), C(4) and C(5) bonds abstraction from the C(4) atom will have the highest dissociation energy limit of 17.65 eV. This value is obtained from the excitation energy of the H($n=4$) states of 12.75 eV and the C-H bond strength of 4.90 eV taken to be equal to that in benzene [23]. The excess energy of 4.25 eV above the dissociation limit (H($n=4$) appearance energy is at 21.9 eV) will appear in internal excitation of the ring isoxazolyl radical and/or in translational energy, mainly of the much lighter H atom. For comparison, in the studies of electron impact dissociation of methane molecules [25], the kinetic energy of the H(n=3) atoms was determined from analysis of Doppler profiles of the H$_\alpha$ line to be 2.8 eV. Also in the photofragmentation of pyrrole molecules, fast H atoms (0.75 eV) with a narrow kinetic energy distribution were found and assigned to a rapid and direct breaking of the N-H bond in the excited repulsive $\pi\sigma^*$ state [2]. A fragmentation energy limit of 15.5 eV, lower than for (5), is estimated for a process proceeding via opening of the isoxazole ring into the linear nitrile N≡CCH$_2$HC=O isomer and elimination of the H atom from C(4) or C(5) which requires 3.90 eV. Here, the higher excess energy of 6.4 eV may, at least partialy, contribute to further fragmentation of the isoxazolyl radical.

The excited states, which by fragmentation give rise to the above species are built on single-hole or single-hole satellite ion cores. Comparison of the measured appearance energies with the known energies of the photoelectron bands enable a tentative

identification of these ion cores. The formation of CH in excited states may correspond to the ionic bands observed in the very recent threshold photoelectron studies in the energy range 14-16 eV [22] which include the $(13a')^{-1}$ and $(12a')^{-1}$ bands. The states dissociating into H(n=4,l) atoms may be attributed to an ionic band detected at 22.95 eV in the photoelectron spectrum [22] while those related to H(n, l) atoms with n=5-7 to two bands at 24.49 eV and 26.44 eV. These states are most likely the higher-lying Rydberg states of isoxazole.

4. Conclusions

Dissociation and fragmentation processes of isoxazole molecules yielding electronically excited neutral atomic and diatomic species have been investigated by the electron impact optical excitation technique. The observed fragmentation products are hydrogen atoms H(n), n=4-7 and the diatomic CH($A^2\Delta$), CN($B^2\Sigma^+$) and C_2($d^3\Pi_g$) molecules. The appearance energies for the H(n=4) and CH($A^2\Delta$) and CN($B^2\Sigma^+$) were determined and compared with estimated fragmentation energy limits to elucidate the possible fragmentation processes. This shows that the above fragments may be released with kinetic energies of up to few electronvolts. Kinetic energy measurements would bring more insight into the dynamics of the processes as would theoretical thermodynamic calculations. The fragmentation processes induced by electron impact in isoxazole may be further extended to for example purine nucleic acid bases, adenine and guanine and other related biomolecules which contain isoxazole ring structure to bring more information that is required in studies of the interaction of secondary electrons produced by primary ionizing radiation in biological media.

Acknowledgements

References

[1] A.L. Sobolewski, W. Domcke, C. Dedonder-Lardeux, C. Jouvet, Phys. Chem. Chem. Phys. 4 (2002) 1093.

[2] J. Wei, J. Riedel, A. Kuczmann, F. Renth, F. Temps, Faraday Discuss. 127 (2004) 267.

[3] M. Barbatti, M. Vazdar, A. J.A. Aquino, M. Eckert-Maksić, H. Lischka, J. Chem. Phys. 125 (2006) 164323.

[4] N. Gavrilov, S. Salzmann, C.M. Marian, Chem. Phys. 349 (2008) 269.

[5] S. Salzmann, M. Kleinschmidt, J. Tatchen, R. Weinkauf, C.M. Marian, Phys. Chem. Chem. Phys. 10 (2008) 380.

[6] R. Weinkauf, L. Lehr, E.W. Schlag, S. Salzmann, C.M. Marian, Phys. Chem. Chem. Phys. 10 (2008) 393.

[7] A. Lifshitz, D. Wohlfeiler, J. Phys. Chem. 96 (1992) 4505.

[8] K. Okada, K. Saito, J. Phys. Chem. 100 (1996) 9365.

[9] J. Higgins, X. Zhou, R. Liu, J. Phys. Chem. A 101 (1997) 7231.

[10] G.E. Davico, J. Phys. Org. Chem. 18 (2005) 434.

[11] G. Bouchoux, Y. Hoppilliard, Org. Mass Spectrom. 16 (1981) 459.

[12] I.C. Walker, M.H. Palmer, J. Delwiche, S.V. Hoffmann, P. Limão-Vieira, N.J. Mason, M.F. Guest, M.-J. Hubin-Franskin, J. Heinesch, A. Giuliani, Chem. Phys. 297 (2004) 289.

[13] M. Dampc, M. Zubek, Int. J. Mass Spectrom. 277 (2008) 52.

[14] J. Gackowska, R. Olszewski, M. Zubek, Rad. Phys. Chem. 68 (2003) 133.

[15] A.F.J. van Raan, J.P. de Jongh, J. van Eck, H.G.M. Heideman, Physica 53 (1971) 45.

[16] I. Humphrey, J.F. Williams, E.L. Heck, J. Phys. B 20 (1987) 367.

[17] M. Tokeshi, K. Nakashima, T. Ogawa, Chem. Phys. 203 (1996) 257, Chem. Phys. 206 (1996) 237.

[18] L. Nemes, M. Mohai, Z. Donko, I. Bertoti, Spectrochim. Acta Part A 56 (2000) 761.

[19] H.A. Bethe, E.E. Salpeter, Quantum Mechanics of One- and Two-Electron Atoms, Plenum Publishing Corporation, New York, 1977, p. 267, Table 16a.

[20] J.M. Marendić, M.D. Tasić, J.M. Kurepa, Chem. Phys. 91 (1984) 273.

[21] S. Tsurubuchi, K. Motohashi, S. Matsuoka,T. Arikawa, Chem. Phys. 155 (1991) 401.

[22] M. Dampc, B. Mielewska, M.R.F. Siggel-King, G.C. King , B. Sivaraman, S.

Ptasińska, N. Mason, M. Zubek, Chem. Phys. 367 (2010) 75.

[23] D.R. Lide (Ed.), CRC Handbook of Chemistry and Physics, CRC Press, Boca Raton, 2004.

[24] I. Linert, M. Dampc, I. Lachowicz, M. Zubek, (2010) to be published.

[25] N. Kouchi, M. Ohno, K. Ito, N. Oda, Y. Hatano, Chem. Phys. 67 (1982) 287.

Figure captions

Fig. 1.

Schematic diagrams of: (a) isoxazole C_4H_3NO, (b) furan C_4H_4O, (c) pyrrole C_4H_4NH and (d) thiophene C_4H_4S molecules. Labeling of the atoms is shown for isoxazole. All molecules have planar geometry in the ground state. Color code: the carbon atom is grey, oxygen atom red, nitrogen atom light blue, sulphur atom yellow, hydrogen atom dark blue.

Fig. 2.

Emission spectrum measured in isoxazole at an incident electron energy of 70 eV. The spectrum was corrected for the wavelength dependence of the sensitivity of the detection system.

Fig. 3.

Line intensity of the Balmer series as a function of the n quantum number. The solid line shows the best fit to the experimental points obtained for the $n^{-3.57}$ dependence.

Fig. 4.

Emission cross section measured for the $CH(A^2\Delta \rightarrow X^2\Pi_r)$ band. The inset shows the threshold region of the excitation. The CH appearance energy is indicated by an arrow.

Fig. 5

Emission cross section of the CN(B$^2\Sigma^+\rightarrow$X$^2\Sigma^+$) band and H$_\beta$ line. The inset shows the

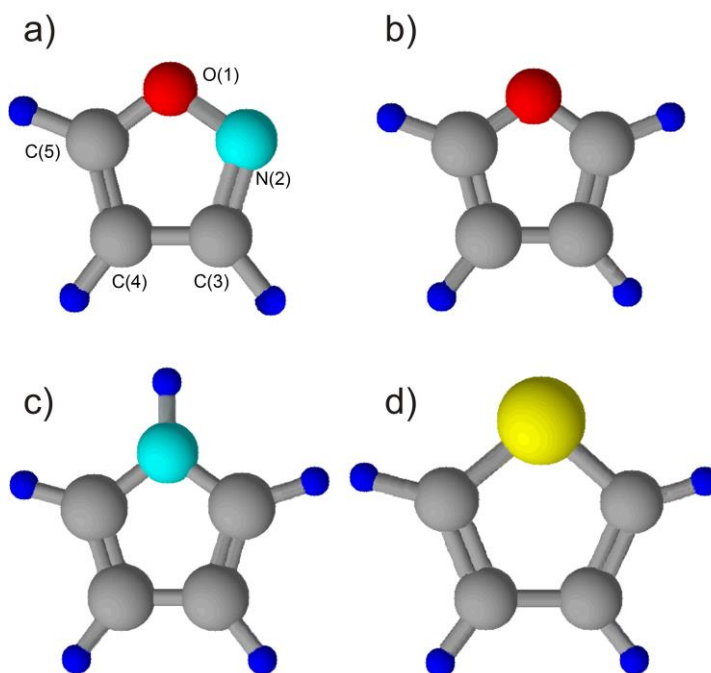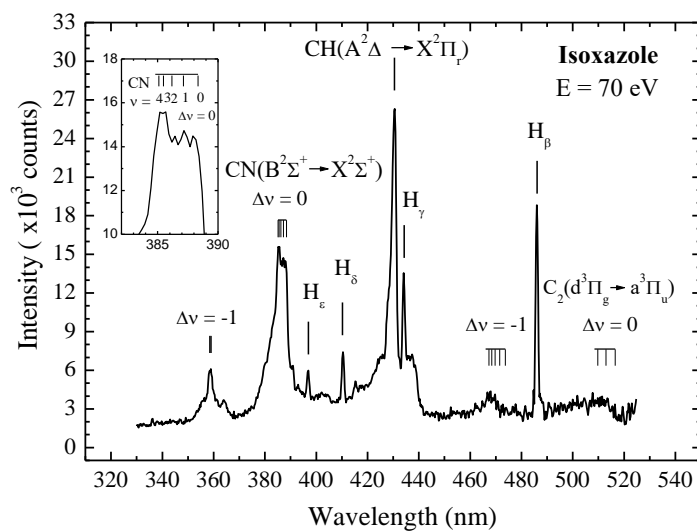threshold region of the CN excitation. The appearance energy is indicated by an arrow.
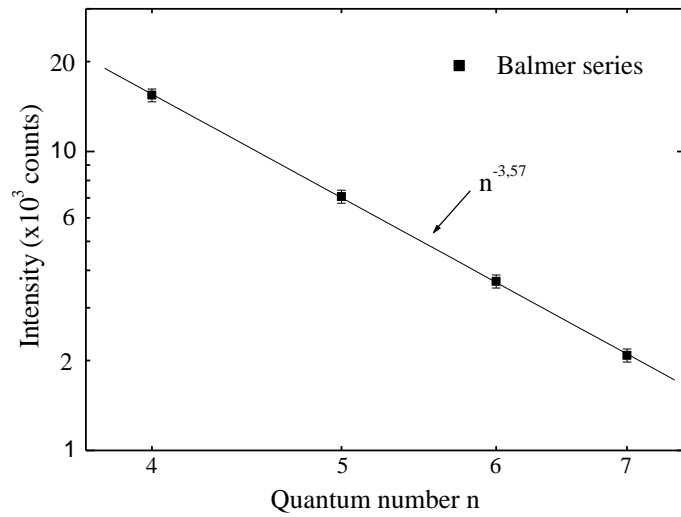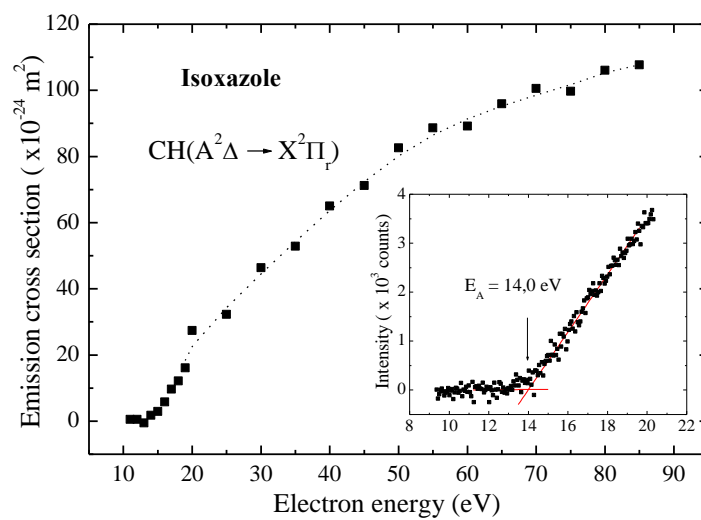

Fig. 1

Fig. 2

Fig.3

Fig. 4

16

Fig. 5